Stem Cell Research (2011) 6, 276–285

available at www.sciencedirect.com

www.elsevier.com/locate/scr

METHODS AND REAGENTS

Differentiation of human embryonic stem cells into pancreatic endoderm in patterned size-controlled clusters

Dennis Van Hoof [a,1], Adam D. Mendelsohn [b,1], Rina Seerke [a], Tejal A. Desai [b,c], Michael S. German [a,c,*]

[a] Diabetes Center, University of California San Francisco, 35 Medical Center Way, San Francisco, CA 94143, USA
[b] Joint Graduate Group in Bioengineering, University of California at San Francisco and University of California at Berkeley, San Francisco, CA 94158, USA
[c] Department of Bioengineering and Therapeutic Sciences, University of California at San Francisco, San Francisco, CA 94158, USA

Received 13 January 2011; received in revised form 22 February 2011; accepted 23 February 2011
Available online 2 March 2011

Abstract Pancreatic β-cells function optimally when clustered in islet-like structures. However, nutrient and oxygen deprivation limits the viability of cells at the core of excessively large clusters. Hence, production of functional β-cells from human embryonic stem cells (hESCs) for patients with diabetes would benefit from the growth and differentiation of these cells in size-controlled aggregates. In this study, we controlled cluster size by seeding hESCs onto glass cover slips patterned by the covalent microcontact-printing of laminin in circular patches of 120 μm in diameter. These were used as substrates to grow and differentiate hESCs first into SOX17-positive/SOX7-negative definitive endoderm, after which many clusters released and formed uniformly sized three-dimensional clusters. Both released clusters and those that remained attached differentiated into HNF1β-positive primitive gut tube-like cells with high efficiency. Further differentiation yielded pancreatic endoderm-like cells that co-expressed PDX1 and NKX6.1. Controlling aggregate size allows efficient production of uniformly-clustered pancreatic endocrine precursors for in vivo engraftment or further in vitro maturation.

Introduction

The elevated blood glucose that characterizes diabetes mellitus results from the loss of insulin-producing β-cells from the islets of Langerhans in the pancreas (type 1 diabetes mellitus) or from a relative deficiency of insulin production in a setting of reduced insulin sensitivity (type 2 diabetes mellitus). Transplantation of cadaveric pancreata or the β-cell-containing islets thereof offers the only cure for patients dependent on exogenous insulin (Shapiro et al., 2000). However, immune-mediated damage to the transplanted β-cells and insufficient revascularization (Lau and Carlsson, 2009) leading to nutrient and oxygen-deprivation, especially inside large islets, limits islet survival. As a consequence, the long-term benefits of these grafts are limited; most recipients remain insulin-independent for less than two years (Ryan et al., 2005). Besides, current numbers of donor organs cannot provide enough material for all patients.

The potential of human embryonic stem cells (hESCs) to differentiate into any somatic cell type, including glucose-

* Corresponding author at: Diabetes Center, University of California San Francisco, 35 Medical Center Way, San Francisco, CA 94143, USA. Fax: +1 415 731 3612.
E-mail address: mgerman@diabetes.ucsf.edu (M.S. German).
[1] These authors contributed equally to this work.

1873-5061/$ – see front matter © 2011 Elsevier B.V. All rights reserved.
doi:10.1016/j.scr.2011.02.004

responsive insulin-producing cells (Kroon et al., 2008), offers a possible solution to the shortage of transplantable cells. Unfortunately, current in vitro differentiation protocols do not generate homogeneous populations of functional β-cells (for review, see Van Hoof et al., 2009a). Furthermore, these protocols rely on consecutive exposures of hESCs to various factors, either in an adherent monolayer format or after an embryoid body-formation step, which is associated with spontaneous differentiation into various undesired cell types. In addition, the size of end-stage clusters varies greatly, and is difficult to control.

The sensitivity of β-cells to external glucose levels, and their responsive insulin release, is highly dependent on cell-cell contact. Notably, clusters comprising multiple β-cells have a greater glucose-stimulated insulin release than single β-cells (Meda et al., 1990; Jaques et al., 2008). Furthermore, β-cells secrete more insulin when in three-dimensional aggregates than in monolayers (Brereton et al., 2006). In addition, nutrient deprivation is observed in transplanted islets with diameters exceeding 100 μm (Lehmann et al., 2007). Therefore, hESC-derived β-cells will most likely function optimally after transplantation when clustered in multicellular structures that are approximately 100 μm in diameter, a size that is large enough for efficient glucose-responsive insulin secretion, yet small enough to prevent nutrient starvation of cells residing in the core.

Here, we report a procedure to derive definitive endoderm cells from hESCs with high efficiency, while culturing them on covalently-bound laminin circular patches of 120 μm in diameter. Subsequent exposure to keratinocyte growth factor converted these adherent aggregates into highly homogeneous clusters comprising mainly HNF1β$^+$ primitive gut tube-like cells. Furthermore, cells in these clusters differentiated into PDX1$^+$/NKX6.1$^+$ pancreatic endoderm upon consecutive exposure to additional factors. In addition, the primitive gut tube-like clusters could be dislodged mechanically, without enzymatic treatment, after which they balled up into uniform ~100 μm-diameter spheres that retained the ability to form pancreatic endoderm-like cells co-expressing PDX1 and NKX6.1. Since the size of transplanted islets impacts insulin secretion and viability (Lehmann et al., 2007), the generation of hESC-derived pancreatic progenitors in spherical clusters of controllable size and cell number could, as proof of concept, contribute to developing a renewable, long-lasting treatment for type I diabetes.

Results

Maintenance of hESCs on laminin-coated glass cover slips

To develop methods for growing hESCs in controlled cluster sizes, we first tested for culturing conditions that allowed for adherence and growth on glass cover slips in the absence of MEFs. Since hESCs have an epithelial character (Van Hoof et al., 2008) and express integrins α2, α6, β1, and β4 (Van Hoof et al., 2006, 2009b; Dormeyer et al., 2008), laminin was chosen for a scaffold protein. Glass cover slips were coated non-covalently with laminin or laminin-containing Matrigel in the absence of MEFs.

Static water contact angle measurements were performed by a technique that assesses the hydrophobicity of a surface to verify laminin attachment. Clean, dry, plasma-treated cover slips are hydrophilic and exhibited water contact angles near zero degrees (n = 3). Laminin or matrigel coating rendered the surfaces more hydrophobic and resulted in water contact angles of 30.7 ± 1.2 and 30.0 ± 1.0, respectively (n = 3). Since laminin is the dominant matrix component of Matrigel, their water contact angles are expected to be similar.

The buoyancy of the generally hydrophobic laminin-coated cover slips was reduced by incubating them overnight in serum-containing medium, which coincidentally increased the affinity of the hESCs for the treated cover slips. Using these laminin-coated surfaces and MEF-conditioned medium supplemented with FGF2, hESCs could be maintained for at least three days without loss of the pluripotency marker OCT4 (Fig. 1). Similar results were obtained with cover slips coated with Matrigel, gelatin, collagen I, or fibronectin (Supplemental Figs. 1A–D); however, cell densities were highest with laminin-coated cover slips. This difference in cell density may have resulted from a higher fraction of cells attaching to the laminin-coated surface than to the Matrigel-coated surface after passaging.

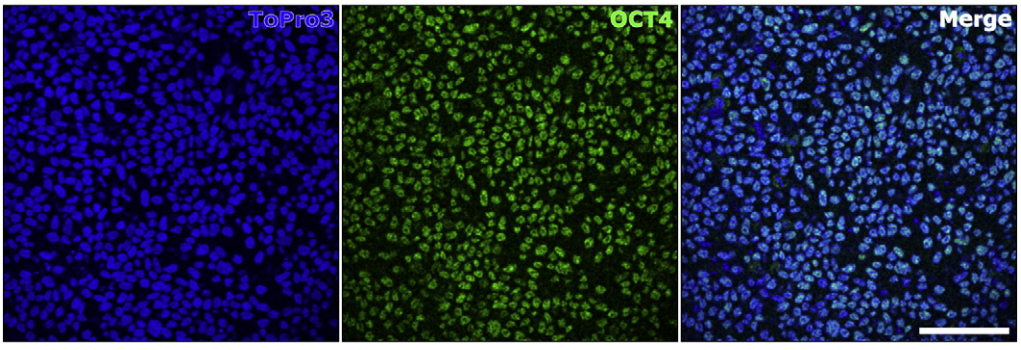

Figure 1 hESCs grown on laminin- or Matrigel-coated glass retain OCT4 expression. Confocal fluorescence microscopic imaging is shown for OCT4 (green) in hESCs that were plated without feeder cells on glass cover slips coated with laminin. Nuclear staining with ToPro3 is shown in blue. Scale bar, 100 μm.

Maintenance of hESCs on microcontact-printed glass cover slips

To control cluster size, glass cover slips were microcontact-printed with covalently-bound laminin in circular patterns of 120 μm in diameter with a spacing of 200 μm in between. Because laminin attachment quenches the aldehydes on the glass surface, and laminin binds poorly to BSA (Mendelsohn et al., 2010), FITC-BSA incubation at 50 μg/ml for 20 min enabled visualization of the unquenched aldehydes on the glass surface between the patterns and confirmed correct laminin patterning (Figs. 2A and B). Finally, to render the glass surface in between the patterns resistant to cell attachment, the remaining aldehydes were then passivated with mPEG-amine. Thorough characterization of cover slips patterned with this method and each step in the functionalization process have been reported previously (Mendelsohn et al., 2010).

After laminin-patterning and mPEG-amine attachment, hESCs were seeded without MEFs on the cover slips at a density of 25,000 cells/cm^2, which corresponds to an effective seeding density of ~28,000 cells per microcontact-printed glass cover slip. After three days in culture, the patches averaged 36.2 cells (SD=11.2, n=86) growing in compact colonies. The cells in these adherent clusters were positive for the pluripotency marker OCT4, but negative for the endoderm marker SOX17 (Figs. 2C and D). When maintained on these laminin patches for more than three days, the cells continued to proliferate (cells in the metaphase and anaphase can be discerned in Fig. 2D, top left panel), forming multi-layered cell aggregates that outgrew the 120 μm circular patches and detached during medium refreshment over the next few days.

Differentiation of hESCs on microcontact-printed glass cover slips

Activin A is known to be a potent component for the differentiation of hESCs into definitive endoderm (D'Amour et al., 2005). First, we tested whether hESCs could differentiate into definitive endoderm when using medium conditioned by activin A-secreting CHO cells (Arai et al., 2006) instead of medium supplemented with purified activin A. Subjecting hESCs that were grown on gelatin-coated

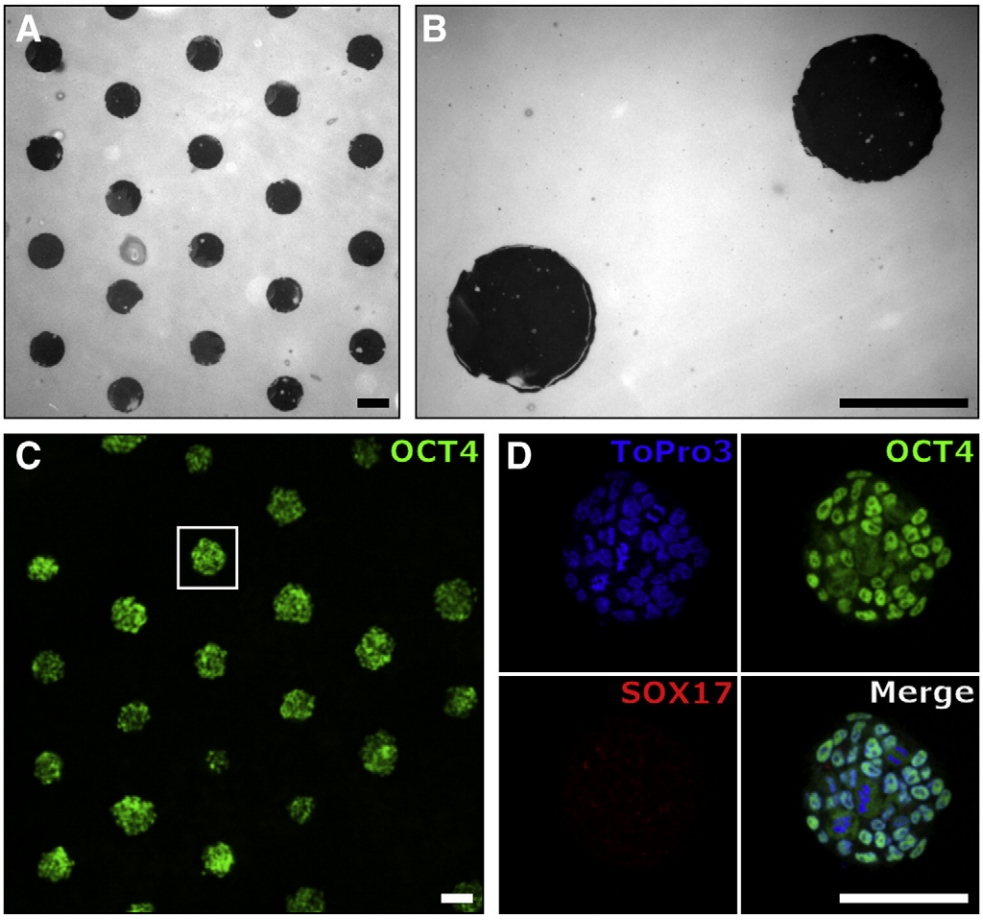

Figure 2 hESCs grown on patches with microcontact-printed laminin retain OCT4 expression. Fluorescence microscopic imaging of FITC-BSA bound to the surface between the microcontact-printed 120 μm-diameter circular laminin patches verifies the pattern organization (A and B). Feeder-free hESCs grown for three days on these laminin-coated patches retained expression of the pluripotency marker OCT4 (C and D, green) but did not express the endoderm marker SOX17 (D, red). Nuclear staining with ToPro3 is shown in blue. Scale bars, 100 μm.

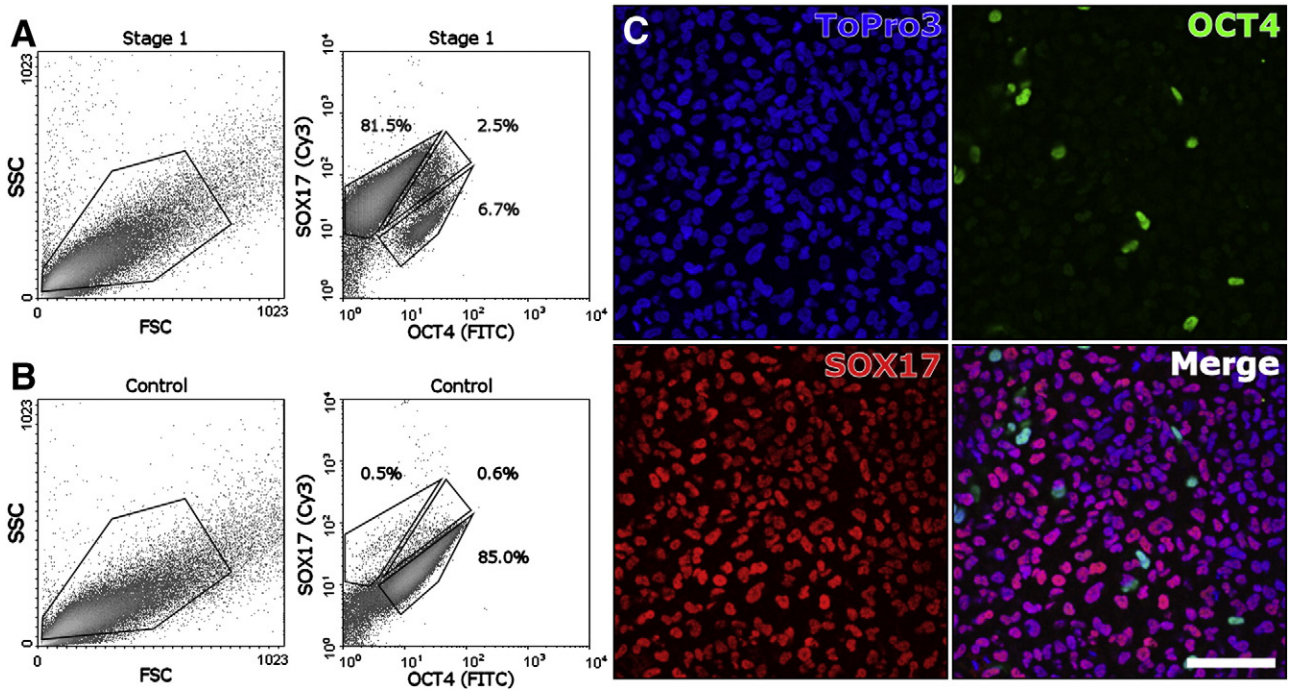

Figure 3 Differentiation of hESCs into definitive endoderm with high efficiency. Flow cytometry analysis of hESCs that were differentiated for three days (A and B) shows that OCT4 expression sharply decreased, and SOX17 emerged, when the hESCs were incubated for three days with medium conditioned by activin A-secreting CHO cells (B). In contrast, OCT4 expression was retained when hESCs were differentiated in unconditioned medium (A). Confocal laser scanning microscopy confirmed the differentiation of the treated cells, showing that only a few cells expressed OCT4 (C, green), while the majority upregulated SOX17 (C, red). (C) Nuclear staining with ToPro3 is shown in blue. Scale bars, 100 μm.

culture plastic to this modified Stage 1 generated definitive endoderm with high efficiency. At the end of day 3, ~84% of the cells stained for the endoderm marker SOX17 (Fig. 3A) as assessed by flow cytometry, and few of these SOX17$^+$ cells (~2.5%) retained high levels of the pluripotency marker OCT4. In contrast, the majority of untreated cells grown under control conditions in unconditioned medium for the same period continued to express high levels of OCT4, and only ~1% expressed SOX17 (Fig. 3B). Analysis of the treated cells by immunofluorescence microscopy confirmed these flow cytometry data, showing rare OCT4$^+$ cells scattered among the SOX17$^+$ majority (Fig. 3C).

RNA expression analysis by real-time RT-PCR confirmed that the hESCs had differentiated into definitive endoderm. After 3 days of treatment, *OCT4* transcript levels fell dramatically (Supplemental Fig. 2A), whereas *SOX17* (Supplemental Fig. 2B) and *FOXA2* (Supplemental Fig. 2C) mRNA levels increased; *SOX7* mRNA levels were very low in hESCs as well as in the differentiated cells (Supplemental Fig. 2D), indicating that the cells had converted to definitive endoderm rather than visceral endoderm.

Since this differentiation procedure efficiently generated definitive endoderm, we applied the same conditions to the hESCs grown on microcontact-printed cover slips 72 h after plating. When subjected to the conditions for Stage 1, all the cells in each adherent cluster expressed SOX17 on the third day, whereas OCT4 staining was reduced to nearly undetectable levels (Fig. 4A).

The Stage 1 cells growing on microcontact-printed cover slips were then sequentially subjected to the succeeding differentiation stages to move them along the pancreatic differentiation lineage. Expression of HNF1β, a marker of the primitive gut tube (i.e. Stage 2), was observed when the cells from Stage 1 were incubated for 3 days with KGF (Fig. 4B). Upregulation of HNF1β was associated with a reduction in SOX17 levels, as has been reported previously (D'Amour et al., 2006). Notably, the liver marker albumin was not detected (inset in Fig. 4B), suggesting that these cells were not committed to the hepatic lineage.

To further differentiate these cells along the pancreatic pathway to Stage 3 cells, they were incubated for 3 days with a combination of (−)-indolactam V, FGF10, BSA-V, and N2 (Chen et al., 2009). Not all the cells positive for HNF1β co-expressed PDX1 at the end of Stage 3 (Fig. 4C), suggesting that only a portion of these cells had adopted posterior foregut-like properties.

During Stage 4, the cells were maintained in B27-containing medium, resulting in the appearance of NKX6.1$^+$ cells among those positive for PDX1 (Fig. 4D). Pancreatic endoderm cells, marked by the co-expression of PDX1 and NKX6.1, were rare and limited to one or two cells per cluster.

Suspension growth and adherence of detached definitive endoderm clusters

Although some clusters remained attached throughout the entire differentiation protocol, the majority detached after Stage 1. The spherical clumps of cells had a uniform diameter of approximately 100 μm (Fig. 5A). When transferred to low-

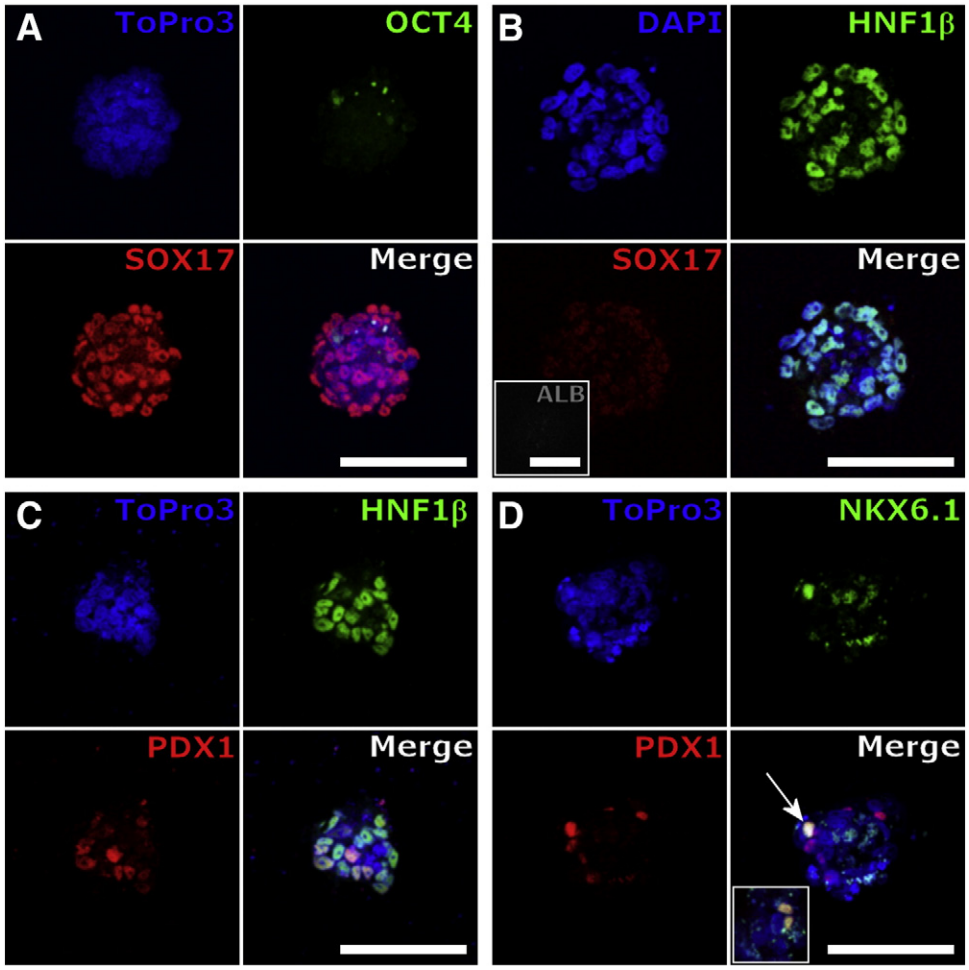

Figure 4 Differentiation of hESCs into pancreatic endoderm on circular laminin-coated patches. Confocal microscopic imaging demonstrates hESCs growth and differentiation on circular laminin-coated patches of 120 μm in diameter (A–D). (A) At Stage 1, the cells differentiated to definitive endoderm, as shown by downregulation of OCT4 (green) and upregulation of SOX17 (red). Most of the cells adopted primitive gut tube-like characteristics by the end of Stage 2 (B), as evidenced by upregulation of HNF1β (green), reduction in SOX17 expression (red), and absence of ALB (inset in bottom-left panel; grey). (C) At Stage 3, some of the HNF1β$^+$ cells (green) co-expressed PDX1 (red), thereby resembling posterior foregut cells. Pancreatic endoderm-like cells, marked by the co-expression of NKX6.1 (green) and PDX1 (red) were seen at Stage 4 (D), and usually occurred as single cells (indicated by an arrow in the bottom right panel) or doublets (inset in bottom right panel) in the clusters. Nuclear staining with ToPro3 (top left, bottom left, and bottom right panels) and DAPI (top right panel) is shown in blue. Scale bars, 100 μm.

attachment culture plates in the conditions used for Stage 2, the cells in these clusters expressed HNF1β (Fig. 5B), as observed for the adherent clusters (Fig. 4B). Three-dimensional analysis revealed that essentially all cells in these spherical structures adopted a primitive gut tube-like identity (Fig. 5C and Supplemental online video 1), suggesting that Stage 2 differentiation in suspension is as efficient as that for adherent cells.

When kept in suspension for an extended time, while proceeding to the subsequent stages, the clusters clumped together, forming larger aggregates of various shapes and sizes. In these suspended clusters, only a few PDX1$^+$ cells were found, some of which were positive for NKX6.1 (Supplemental Fig. 3). On the other hand, when the suspended definitive endoderm clusters were allowed to adhere, and were exposed to the conditions for Stage 3 for

Figure 5 Suspension differentiation of hESCs into primitive gut tube cells, and into posterior foregut cells after replating. (A) A bright-field microscopic image is shown of differentiating clusters that dislodged spontaneously after Stage 1. (B) Confocal microscopic images are shown at Stage 2 of a suspended cluster, all cells of which express HNF1β (green) and low levels of SOX17 (red). (C) Side views of a 3-D reconstruction of a cluster similar to that shown in (B); the arrows aimed at the sphere indicate the point of view. (D) A confocal microscopic image is shown of a cluster that was plated at the onset of Stage 3 after having been in suspension during Stage 2. Like others, cells from this cluster express HNF1β (green), with PDX1$^+$ cells (red) at the center of the colony-like structure. Nuclear staining with ToPro3 is shown in blue. Scale bars, 100 μm.

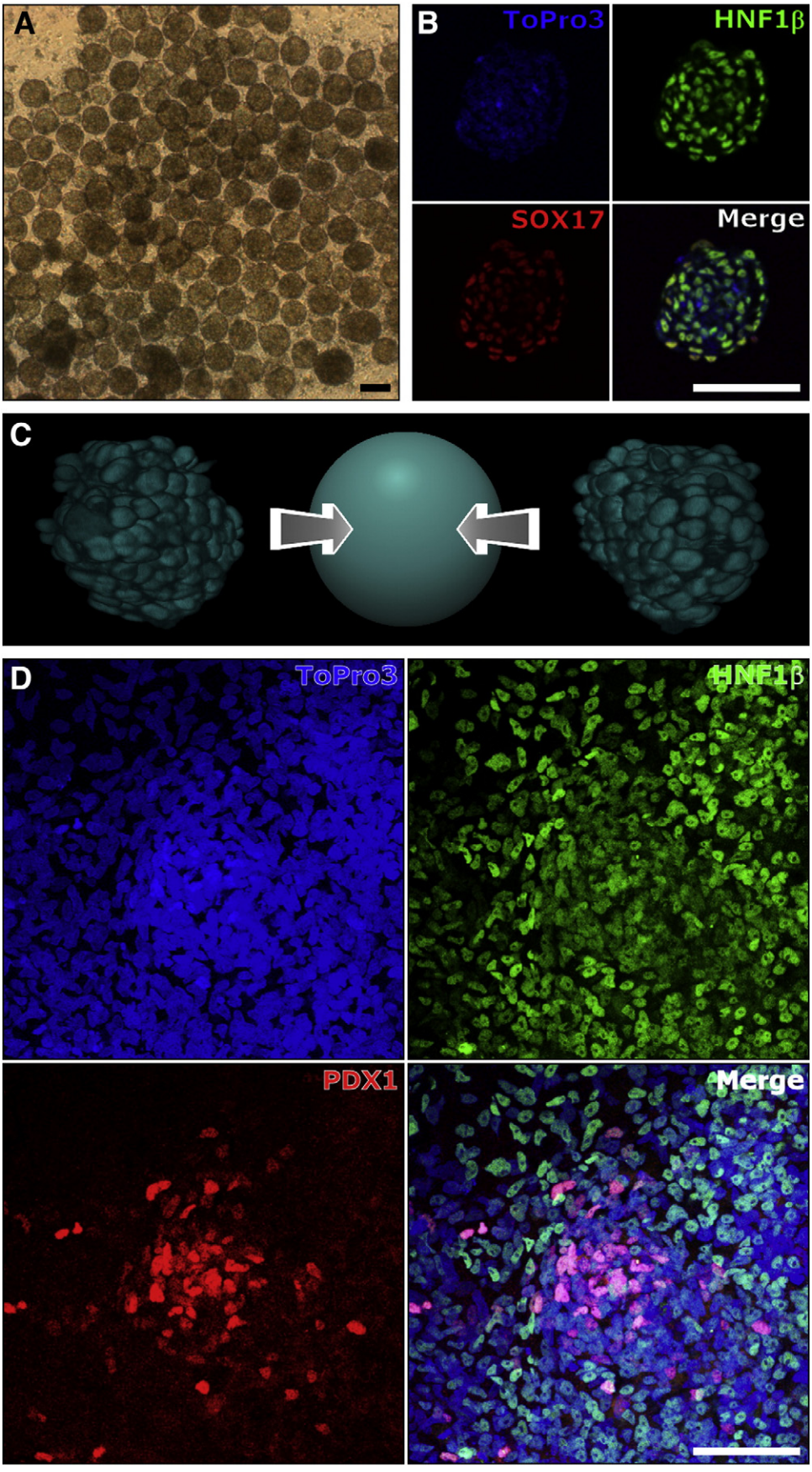
A
B
ToPro3
HNF1β
SOX17
Merge
C
D
ToPro3
HNF1β
PDX1
Merge

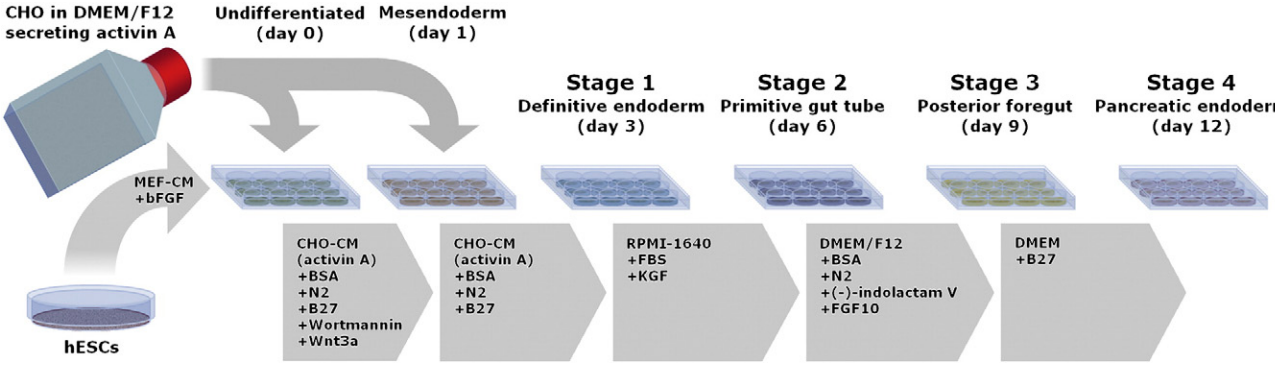

Figure 6 Differentiation of hESCs. Schematic overview of the differentiation procedure as described in the Materials and methods section.

three days, PDX1$^+$ posterior foregut-like cells were localized at the centers of the newly adherent clusters (Fig. 5D), and were surrounded by an HNF1β^+ monolayer. PDX1$^+$ cells residing in this HNF1β^+ monolayer were scattered as single cells or pairs, with the highest density close to the center. Notably, these adherent clusters adopted a colony-like architecture and had lost their original 100 μm-diameter spherical shape.

Discussion

After the demonstration of efficient formation of definitive endoderm (D'Amour et al., 2005) and pancreatic endocrine cells from hESCs, efforts have been focused on improving the yield and purity of β-cell-like derivatives, resulting in diverse protocols for generating insulin-producing cells (for reviews, see Van Hoof et al., 2009a; Mfopou et al., 2010). However, these insulin-producing cells differentiated in vitro from hESCs do not secrete insulin in response to glucose as normal β-cells do, and share characteristics with a terminal lineage of pancreatic endocrine cells seen early in normal pancreatic development. Only when transplanted at the pancreatic endoderm-equivalent stage (Stage 4) and maintained for several months, do in vitro-generated endocrine precursors mature into glucose-responsive insulin-secreting cells exhibiting characteristics of true β-cells (Kroon et al., 2008). The failure of the in vitro protocols to generate true β-cells could result from the absence of interacting cells from other lineages (mesoderm and ectoderm) present in the developing pancreatic bud during normal embryonic development of the pancreas. Remarkably, the site of transplantation did not make any substantial difference in the efficacy of pancreatic endoderm maturation (Kroon et al., 2008), thus, a process as simple as vascularization might be sufficient to allow the generation of glucose responsive β-cells.

Although the site of transplantation may not have been critical, the size of transplanted cell clusters was, since 150×150 μm chunks of in vitro-generated pancreatic endoderm gave optimal generation of physiologically regulated β-cells in the transplantation model (Kroon et al., 2008). In line with this observation, aggregated β-cells release insulin more efficiently than do isolated β-cells (Meda et al., 1990; Jaques et al., 2008), and they secrete more insulin from three-dimensional aggregates as opposed to single layers of cells (Brereton et al., 2006). The optimal cluster size for the differentiation of functional β-cells from hESC-derived pancreatic endoderm-like cells, while avoiding the starvation of cells at the core, needs to be determined. Control of cluster size can be achieved through the patterning of a variety of materials, such as PVA (Cheng and LeDuc, 2006), alkanethiolates (Mrksich et al., 1997), and laminin (Mendelsohn et al., 2010). We tested several shapes (squares and circles), sizes (ranging from 40 to 120 μm), arrangements (square grid and triangular alignment), and distances between the patches. We found that, if the patch surface was too small, the number of cells that could adhere to the laminin competed for space; as a result, the cell aggregates became multilayered and easily detached from the patches during medium refreshment. On the other hand, larger patches, generating clusters of more than 100 μm in diameter, were not desirable as pointed out above. Furthermore, if the distance between the patches became too small, the cells were able to bridge the PEGylated spaces in between. In the end, 120-micron circles with 200-μm-gaps in a triangular arrangement proved optimal. Our studies here demonstrate the feasibility of controlling cell number as well as colony shape and pattern, using covalently patterned laminin, before initiating an in vitro differentiation procedure. Moreover, this system readily allows further optimization and adjustment of growth conditions (e.g. oxygen levels, media additives, growth factors, etc.).

Transplantation of pancreatic endoderm generated from hESCs or induced pluripotent cells with subsequent differentiation to mature β-cells in vivo could be considered for the treatment of diabetes in humans. However, our current laboratory setting for generating cell clusters on microcontact-printed surfaces would be difficult to expand sufficiently to generate enough cells for human trials. In addition to scale-up, preventing massive detachment of the aggregates during the differentiation process would increase the yield of transplantable material significantly. The reduced affinity of the differentiating aggregates for the microcontact-printed substrate may result from changes in the range of anchoring proteins, such as integrins, expressed as the cells undergo further differentiation. Knowledge of the attachment proteins expressed by these cells could be used with the microcontact-printed method to generate ideally constituted and patterned growth surfaces.

Cell detachment may also result from a weakening of the laminin from the glass cover slip. Previously, Fourier

transform infrared characterization on cover slips that were patterned using this method verified the attachment of laminin to the underlying aldehyde. However, in-depth analysis of the spectrum revealed a significant spike, which represents an amine, suggesting that multiple layers of laminin had attached (Mendelsohn et al., 2010). As a result, while a portion of the laminin had bound covalently, the rest could have attached through weaker interactions. Although to a lesser extent than was found in this study, we have observed 832–13 insulinoma cells detaching from microcontact-printed laminin after several days in cell culture conditions, and found that overlaying with low-melting point agarose or other gels could hold the cells in place (data not shown). However, these gels adhere poorly to the PEGylated glass surface, and limit the diffusion of large molecules, like growth factors. Alternatively, a protocol that allows efficient differentiation in suspension once definitive endoderm has been formed would overcome this problem entirely.

Conclusion

We have shown the utility of controlling cell cluster size in differentiating hESCs into definitive endoderm and primitive gut tube-like cells with high efficiency, and subsequent differentiation into pancreatic endoderm. To do so, we microcontact-printed patches of laminin onto glass cover slips to serve as an attachment and growth substrate for the hESCs. Optimization and scale-up of this process might yield enough tissue for transplantation studies in diabetic mouse models. Controlling cluster size promises to produce a cellular architecture that enables sufficient nutrient availability as well as physiological insulin secretion. Microcontact-printing provides a feasible approach to the production of cell clusters of desired size for both optimal production and post-transplantation function.

Materials and methods

Cleaning of glass cover slips

Glass cover slips were sonicated in a 70:30 ethanol:Milli-Q water (Millipore, Bedford MA) solution for 10 min, then dried with N_2. Following this, cover slips were cleaned in oxygen plasma at 175–200 W and 0.5 mTorr for 30 s (Plasmaline, TCGAL Corporation).

Coating of cover slips

Clean dry plasma-treated glass cover slips were incubated with 20 μg/ml Matrigel (BD Biosciences), mouse laminin (Invitrogen), porcine gelatin (Sigma), rat tail collagen I (Sigma) or human plasma fibronectin (Gibco) for 30 min. Cover slips were then sonicated in phosphate-buffered saline (PBS) for 5 min, rinsed with Milli-Q water and dried with N_2.

Preparation of aldehyde-terminated glass cover slips

Clean, dry, plasma-treated glass cover slips were silanized in a freshly prepared solution of 2% APTES (v/v) in 95:5 ethanol:Milli-Q water for 30 min, followed by 10 dips in a freshly prepared solution of 70:30 ethanol:Milli-Q water. The cover slips were then submerged in a second freshly prepared solution of 70:30 ethanol:Milli-Q water and sonicated for 20 s. Cover slips were dried with N_2, and transferred to a glass petri dish on a hot plate set to 120 °C for 1 h. The cover slips were kept in a vacuum chamber at room temperature for at least 24 h before use. The amine-terminated cover slips were sonicated for 10 min in 70:30 ethanol:Milli-Q water before incubation for 1 h at room temperature in 10% glutaraldehyde in PBS. The aldehyde-terminated cover slips were sonicated for another 10 min in 70:30 ethanol:Milli-Q water, and then dried with a stream of N_2.

Preparation of polydimethylsiloxane (PDMS) stamps for microcontact printing of laminin

PDMS stamps were fabricated through a multi-step process that uses photolithography and micropatterning techniques. First, a negative photoresist SU-8 2010 was spin cast onto a silicon wafer at 2000 rpm for 1 min, yielding a thickness of approximately 13 μm as determined by profilometry (Ambios XP-2, Ambiostech, Santa Cruz, CA). SU-8 films were pre-baked on a hot-plate at 95 °C for 3 min. SU-8 films were subsequently patterned by exposure to UV light through a transparency mask defining 120 μm circles in a triangularly-packed formation with 200 μm spacing in between the edges of each pattern. Patterned SU-8 films were post-baked at 95 °C for 4 min and then immersed in SU-8 developer for 2 min to remove SU-8 that had not been crosslinked. Wafers were subsequently rinsed with SU-8 developer, isopropyl alcohol, and dried with a stream of N_2. Last, the wafers were baked at 150 °C for 15–20 min.

An inverse pattern of the silicon wafer was prepared with PDMS. The base and curing agent were mixed at a 10:1 by mass and deposited onto the micropatterned wafers. The PDMS film was then de-gassed under vacuum for 1–2 h to remove all bubbles, and cured at 70 °C for at least 2 h at atmospheric pressure. Once cured, the PDMS was cut and peeled from the silicon master.

Covalent attachment of laminin by microcontact printing

Following exposure of PDMS stamps to O_2 plasma for 30 s at 175–200 W and 0.5 mTorr, the surface was covered with a solution of 200 μg/ml mouse laminin (1 mg/ml; Invitrogen) in PBS and incubated for 30 min at room temperature. A Kimwipe was used to wick away excess solution before drying the remaining liquid with N_2. Immediately after drying, the PDMS stamps were carefully placed on the aldehyde-terminated cover slip with a 10 g weight for 30 min at room temperature. The stamps were carefully peeled off, leaving printed laminin.

Covalent attachment of PEG

After PDMS stamping of laminin, the cover slips were covered with 25 μl of 3 mM mPEG-amine in methanol and excess sodium cyanoborohydride (>8 mM) to quench unreacted aldehyde groups. Cover slips were incubated for >12 h in a chemical fume hood to vent hydrogen cyanide gas,

subsequently sonicated for 5 min in methanol, and rinsed with methanol before being dried with N_2.

Fluorescent imaging of cover slips

Cover slips that had been printed with laminin were exposed to a 50 μg/ml fluorescein isothiocyanate-bovine serum albumin (FITC-BSA) solution before PEG functionalization for 20 min, sonicated in PBS for 5 min, rinsed with Milli-Q water, and dried with N_2. Images were taken with a wide-field fluorescent microscope (Olympus BX60).

hESC culture and differentiation

Undifferentiated CyT49 hESC were grown as described previously (D'Amour et al., 2006) with minor modifications to the original protocol. The day before passaging hESCs, mitomycin-C-treated mouse embryonic fibroblast feeder cells (MEFs; Millipore Specialty Media) were plated onto gelatin-coated (Sigma-Aldrich) 60 mm dishes (Falcon) at a density of 5000 cells/cm^2. Biweekly, the hESCs were passaged enzymatically with Accutase (Esgro) according to the manufacturer's protocol, and seeded at a density of 50,000–100,000 cells/cm^2. Daily, the hESCs received fresh hESC medium that was supplemented with 10 ng/ml FGF2 (R&D Systems), but did not contain activin A. Differentiation was conducted in 12-well plates (Falcon) that contained the microcontact-printed glass cover slips (Fisherbrand) described above (Fig. 6). Prior to differentiation, the hESCs were seeded at a density of 25,000 cells/cm^2 in MEF-conditioned hESC medium supplemented with 10 ng/ml FGF2, and washed once with PBS 72 h post passaging. Differentiation into definitive endoderm was carried out using DMEM/F12 that was conditioned by CHO cells secreting recombinant activin A (Arai et al., 2006). For the first 24 h, this conditioned medium was supplemented with 2 mg/ml bovine serum albumin fraction V (BSA-V; Sigma), 0.5×N2 and 0.5×B27 medium supplements (Invitrogen), 50 ng/ml Wnt3a (R&D Systems), and 100 nM wortmannin (Sigma). Subsequently, the differentiating cells were incubated for an additional 48 h in the medium described above, without wortmannin and Wnt3a. To generate primitive gut tube-like tissue, the cells were incubated for 72 h in RPMI 1640 (Invitrogen) with 2% (vol/vol) FBS (VWR Hyclone) and 50 ng/ml KGF. For the generation of posterior foregut tissue, cells at the primitive gut tube stage were incubated for 72 h in DMEM/F12 with 1×N2, 300 nM (−)-indolactam V (Calbiochem), 2 mg/ml BSA-V, and 10 ng/ml FGF10 (R&D Systems). To generate pancreatic endoderm, the posterior foregut cells were incubated for 72 h in DMEM (Invitrogen) with 1×B27. Where indicated, the definitive endoderm-like aggregates were dislodged from the microcontact-printed cover slips by pipetting, transferred to low-attachment 12-well plates (Falcon) to keep them in suspension, and subjected to the differentiation procedure described above. All media were refreshed daily.

Immunofluorescence microscopy

Cells were fixed and stained as described previously (Van Hoof et al., 2009b), using the primary antibodies mouse anti-OCT4 (1:200; Santa Cruz), goat anti-SOX17 (1:1000, R&D Systems), rabbit anti-HNF1b (1:100, Santa Cruz), mouse anti-ALB (1:500, Sigma-Aldrich), goat anti-PDX1 (1:10,000, Abcam), and mouse anti-NKX6.1 (1:50, Hybridoma F55A10-c), in combination with the secondary antibodies FITC-conjugated donkey anti-mouse, Cy3-conjugated donkey anti-goat, FITC-conjugated donkey anti-rabbit (all 1:200, Jackson ImmunoResearch Inc), and Alexa Fluor 647-conjugated donkey anti-mouse (1:200, Invitrogen Life Technologies). The cells were counter-stained with DAPI (Roche) or ToPro3 (Invitrogen Life Technologies) and mounted in VectaShield (Vector Laboratories Inc). Images were captured using SL and SP2 confocal laser scanning microscopes (Leica Microsystems), and processed with Paint Shop Pro XI (Corel) and ImageJ 1.43u to reconstruct the three-dimensional (3-D) image of the cluster shown in Fig. 5C and Supplemental online video 1.

Flow cytometry

Cells were trypsinized and fixed as described (Van Hoof et al., 2006), and permeabilized for 15 min in PBS with 0.4% Triton X-100 and 1% BSA (Sigma-Aldrich). Then, the cells were stained with the primary and secondary antibodies indicated above, and sorted using an LSR II Flow cytometer (BD Biosciences). The data were obtained with FACSDiva 6.1.3 (BD Biosciences), and processed with WinMDI 2.9.

Quantitative real-time PCR

hESCs and definitive endoderm cells were collected from 12-well plates (Falcon). RNA was extracted using TRIzol reagent (Invitrogen). Concentrations of total RNA were measured using the NanoDrop ND-1000 Spectrophotometer (NanoDrop Technologies Inc), and 300–500 ng of this RNA was used in a reverse transcription (RT) reaction with a Superscript III cDNA Synthesis kit (Invitrogen). SYBR Green master mix (Qiagen) RT-PCR reactions were set up in duplicate using 300–500 ng cDNA with 300 nM forward and reverse primers summarized in Table 1 in an Applied Biosystems 7900. Relative expression values were normalized relative to the housekeeping gene *GUSB*, and the values from the definitive endoderm samples were compared to those of the undifferentiated hESCs.

Supplementary materials related to this article can be found online at doi:10.1016/j.scr.2011.02.004.

Table 1 RT-PCR primers.

OCT4	Forward: 5′-TGG GCT CGA GAA TGT G-3′
	Reverse: 5′-GCA TAG TCG CTG CTT GAT CG-3′
SOX7	Forward: 5′-ACG CCG AGC TCA GCA AGA T-3′
	Reverse: 5′-TCC ACG TAC GGC CTC TTC TG-3′
SOX17	Forward: 5′-GGC GCA CGA GAA TCC AGA-3′
	Reverse: 5′-CCA CGA CTT GCC CAG CAT-3′
FOXA2	Forward: 5′-GGG AGC GGT GAA GAT GGA-3′
	Reverse: 5′-TCA TGT TGC TCA CGG AGG AGT A-3′
GUSB	Forward: 5′-ACG CAG AAA ATA TGT GGT TGG A-3′
	Reverse: 5′-GCA CTC TCG TCG GTG ACT GTT-3′

Disclosure of potential conflicts of interest

The authors declare no potential conflicts of interest.

Acknowledgments

This work was supported by the California Institute for Regenerative Medicine and the Juvenile Diabetes Research Foundation (JDRF grant awards 3-2008-477, 35-2008-628, and 1-2010-152).

References

Arai, K.Y., Tsuchida, K., Li, C., Watanabe, G., Sugino, H., Taya, K., Nishiyama, T., 2006. Purification of recombinant activin A using the second follistatin domain of follistatin-related gene (FLRG). Protein Expr. Purif. 49, 78–82.

Brereton, H.C., Carvell, M.J., Asare-Anane, H., Roberts, G., Christie, M.R., Persaud, S.J., Jones, P.M., 2006. Homotypic cell contact enhances insulin but not glucagon secretion. Biochem. Biophys. Res. Commun. 344, 995–1000.

Chen, S., Borowiak, M., Fox, J.L., Maehr, R., Osafune, K., Davidow, L., Lam, K., Peng, L.F., Schreiber, S.L., Rubin, L.L., Melton, D., 2009. A small molecule that directs differentiation of human ESCs into the pancreatic lineage. Nat. Chem. Biol. 5, 258–265.

Cheng, C.M., LeDuc, P.R., 2006. Micropatterning polyvinyl alcohol as a biomimetic material through soft lithography with cell culture. Mol. Biosyst. 2, 299–303.

D'Amour, K.A., Agulnick, A.D., Eliazer, S., Kelly, O.G., Kroon, E., Baetge, E.E., 2005. Efficient differentiation of human embryonic stem cells to definitive endoderm. Nat. Biotechnol. 23, 1534–1541.

D'Amour, K.A., Bang, A.G., Eliazer, S., Kelly, O.G., Agulnick, A.D., Smart, N.G., Moorman, M.A., Kroon, E., Carpenter, M.K., Baetge, E.E., 2006. Production of pancreatic hormone-expressing endocrine cells from human embryonic stem cells. Nat. Biotechnol. 24, 1392–1401.

Dormeyer, W., Van Hoof, D., Braam, S.R., Heck, A.J., Mummery, C.L., Krijgsveld, J., 2008. Plasma membrane proteomics of human embryonic stem cells and human embryonal carcinoma cells. J. Proteome Res. 7, 2936–2951.

Jaques, F., Jousset, H., Tomas, A., Prost, A.L., Wollheim, C.B., Irminger, J.C., Demaurex, N., Halban, P.A., 2008. Dual effect of cell–cell contact disruption on cytosolic calcium and insulin secretion. Endocrinology 149, 2494–2505.

Kroon, E., Martinson, L.A., Kadoya, K., Bang, A.G., Kelly, O.G., Eliazer, S., Young, H., Richardson, M., Smart, N.G., Cunningham, J., Agulnick, A.D., D'Amour, K.A., Carpenter, M.K., Baetge, E.E., 2008. Pancreatic endoderm derived from human embryonic stem cells generates glucose-responsive insulin-secreting cells in vivo. Nat. Biotechnol. 26, 443–452.

Lau, J., Carlsson, P.O., 2009. Low revascularization of human islets when experimentally transplanted into the liver. Transplantation 87, 322–325.

Lehmann, R., Zuellig, R.A., Kugelmeier, P., Baenninger, P.B., Moritz, W., Perren, A., Clavien, P.A., Weber, M., Spinas, G.A., 2007. Superiority of small islets in human islet transplantation. Diabetes 56, 594–603.

Meda, P., Bosco, D., Chanson, M., Giordano, E., Vallar, L., Wollheim, C., Orci, L., 1990. Rapid and reversible secretion changes during uncoupling of rat insulin-producing cells. J. Clin. Invest. 86, 759–768.

Mendelsohn, A.D., Bernards, D.A., Lowe, R.D., Desai, T.A., 2010. Patterning of mono- and multilayered pancreatic beta-cell clusters. Langmuir 26, 9943–9949.

Mfopou, J.K., Chen, B., Sui, L., Sermon, K., Bouwens, L., 2010. Recent advances and prospects in the differentiation of pancreatic cells from human embryonic stem cells. Diabetes 59, 2094–2101.

Mrksich, M., Dike, L.E., Tien, J., Ingber, D.E., Whitesides, G.M., 1997. Using microcontact printing to pattern the attachment of mammalian cells to self-assembled monolayers of alkanethiolates on transparent films of gold and silver. Exp. Cell Res. 235, 305–313.

Ryan, E.A., Paty, B.W., Senior, P.A., Bigam, D., Alfadhli, E., Kneteman, N.M., Lakey, J.R., Shapiro, A.M., 2005. Five-year follow-up after clinical islet transplantation. Diabetes 54, 2060–2069.

Shapiro, A.M., Lakey, J.R., Ryan, E.A., Korbutt, G.S., Tot, E., Warnock, G.L., Kneteman, N.M., Rajotte, R.V., 2000. Islet transplantation in seven patients with type 1 diabetes mellitus using a glucocorticoid-free immunosuppressive regimen. New Engl. J. Med. 343, 230–238.

Van Hoof, D., Passier, R., Ward-Van Oostwaard, D., Pinkse, M.W., Heck, A.J., Mummery, C.L., Krijgsveld, J., 2006. A quest for human and mouse embryonic stem cell-specific proteins. Mol. Cell. Proteomics 5, 1261–1273.

Van Hoof, D., Braam, S.R., Dormeyer, W., Ward-van Oostwaard, D., Heck, A.J., Krijgsveld, J., Mummery, C.L., 2008. Feeder-free monolayer cultures of human embryonic stem cells express an epithelial plasma membrane protein profile. Stem Cells 26, 2777–2781.

Van Hoof, D., D'Amour, K.A., German, M.S., 2009a. Derivation of insulin-producing cells from human embryonic stem cells. Stem Cell Res. 3, 73–87.

Van Hoof, D., Muñoz, J., Braam, S.R., Pinkse, M.W., Linding, R., Heck, A.J., Mummery, C.L., Krijgsveld, J., 2009b. Phosphorylation dynamics during early differentiation of human embryonic stem cells. Cell Stem Cell 5, 214–226.